Elementary excitations and nonlinear dynamics of a magnetic domain wall

V. S. Gornakov, V. I. Nikitenko, I. A. Prudnikov, and V. T. Synogach
Institute of Solid State Physics, Russian Academy of Sciences, Chernogolovka, Moscow District 142432, Russia
(Received 6 January 1992)

Two-dimensional magnons localized in the polarized 180° Bloch domain wall and its nonlinear dynamics at high ac drive field in an yttrium iron garnet single-crystal plate are investigated. The interaction between translational and flexural modes of the wall vibration is studied in detail. The excitation spectrum of the moving wall is shown to depend on its velocity. An unexpected asymmetric dependence of flexural mode eigenfrequencies and resonance linewidths on the wall velocity is found. The flexural waves themselves are found to influence the amplitude of the translational wall vibrations. Two kinds of instability were found at increasing drive field. The first is the transition from the periodic linear vibrations at low field and low wall mobility to weakly nonharmonic oscillations at high mobility. They are shown to be due to the excitation of the standing flexural modes of the wall. And the second one is the transition to the region of chaotic wall motion and low mobility at the highest field studied. The real-time signals, spectral data, and phase-space patterns corresponding to different regions were obtained. The phase portrait at the highest field studied is found to be of the chaotic attractor type.

I. INTRODUCTION

Spin-wave theory is known to be very useful in the description of the basic properties of magnetized crystals.[1,2] The most popular material in spin-wave experiments is yttrium iron garnet (YIG) because of its extraordinarily low ferromagnetic resonance (FMR) linewidth and spin-wave damping even at room temperature. In recent years, due to the growing interest in the chaotic dynamics of nonlinear systems, it also became an important system for investigations in spin-wave instability experiments.[3]

Apart from magnons, magnets may contain domain walls with complicated internal structure, and they, naturally, are expected to affect the total excitation spectrum of the crystal.[4-12] A consistent account of the interactions of different types of wall excitations, magnons, solitons, Bloch lines, and points is therefore important in the description of the relaxation and magnetization dynamics in magnets with domain walls. Some of these excitations, namely, wall magnons with the wave vector $\mathbf{k}$ normal to the magnetization in domains $\mathbf{M}$, according to the theories[6,8-11] have the unusual asymmetric dispersion relation $\omega(\mathbf{k}) \neq \omega(-\mathbf{k})$ (ω is the magnon frequency).

The two lower resonances of the flexural domain-wall oscillations related to the nonuniform distribution of the internal magnetic field in bubble garnet films have been observed in Ref. 13. A more detailed experimental study of the wall-excitation spectrum was carried out on YIG.[14,15] These observations of the excitation of the wall standing flexural waves ($\mathbf{k} \perp \mathbf{M}$) allowed the determination of the wall magnon damping, dispersion, and phase velocity as well as the influence of the Bloch lines. The possibility of a direct study of the magnon spectrum of the moving wall was reported in Ref. 16. In the earlier experiments on the same samples, the chaotic generation of the nonlinear solitonlike excitations of the wall structure in the initially polarized wall was found to occur at high amplitude h_0 of the ac field $h \| \mathbf{M}$.[17,18] Here we present the results of further investigations of the wall magnon spectrum in a wide frequency range (to 60 MHz) and discuss the problem of the excitation of standing waves for the case of asymmetric dispersion (Sec. II). In Sec. III the data are given on the magnon spectra of the wall moving at different velocities, including a possible manifestation of the asymmetry mentioned. The opposite effect of the wall flexural waves' influence on its translational motion is also discussed. Finally, we shall describe instabilities of the wall flexural waves, chaotic wall motion and its dynamic structure conversion occurring at higher h_0.

II. ELEMENTARY EXCITATIONS IN THE POLARIZED DOMAIN WALL

Domain walls in magnets are known to lead to additional localized modes of magnetic excitations. According to this theory, there can exist various branches of these surface excitations of different physical origin.[8,11,19] Here we shall be concerned only with the lower Goldstone branch: the flexural mode of the wall excitations, or so-called Winter's magnons. In the small anisotropy easy-axis ferromagnets, they were predicted to obey the unusual asymmetric dispersion relation [8]

$$\omega(k) = -c_0 k Q^{-1/2} + c_0 |k| (1+Q^{-1})^{1/2}, \quad |k\Delta| \ll 1, \ \mathbf{k} \perp \mathbf{M} \qquad (1)$$

$$\Delta^2 = A/K, \quad c_0^2 = 8\pi A \gamma^2, \quad Q = K/2\pi M^2$$

(A and K are the exchange and anisotropy constants; γ is the gyromagnetic ratio).

In a magnet of finite dimensions the quantization, or the resonant condition of the standing waves, has the fol-

 ©1992 The American Physical Society

lowing form:

$$(k_+ + k_-)d = 2\pi n, \quad n = 0,1,2,\ldots \tag{2}$$

or using Eq. (1) we obtain, as in [10],

$$\omega_n = c\pi n/d = c_0(1+Q^{-1})^{-1/2}\pi n/d\ , \qquad (2c)^{-1} = c_+^{-1} + c_-^{-1},\quad c_\pm = \omega/k_\pm\ , \tag{3}$$

where d is the sample thickness along the axis $OX \| \mathbf{M}$ (Fig. 1); $c_\pm$ are the phase velocities of the backward and forward waves. In this case, of the standing waves with x dependence of the nth mode of the wall displacements differing from the usual sinusoidal, one should be realized:

$$q_n(x,t) \sim \sin(\omega t - k_+ x) + \sin(\omega t - k_- x) = 2\sin\left[\omega t - \frac{\pi n x}{d}(1+Q)^{-1/2}\right]\cos\left[\frac{\pi n x}{d}\right]. \tag{4}$$

This expression obeys the boundary conditions

$$\frac{dq}{dt} + c_0 Q^{1/2}\frac{dq}{dx} = 0, \quad \text{at } x = 0,d\ , \tag{5}$$

which are equivalent to the free boundary conditions only at $Q \gg 1$.

Unlike the previous magneto-optic experiments on YIG [14,15], in the present study of such standing waves a more sensitive and broadband inductive technique has been used. A rectangular YIG sample $10\times0.3\times0.04$ mm^3 in size contained a single domain wall polarized by a dc field $\mathbf{H}_x \perp \mathbf{M}$ (see Fig. 1). The flexural vibration modes of the wall excited by a spatially uniform ac field $\mathbf{h} \| \mathbf{M}$ were detected by a small carefully compensated pickup coil, which was wound directly on the sample. The signal from the coil was fed to the spectrum analyzer, its frequency sweep and additional signal storage and averaging being controlled by a personal computer. Note that we held the value of h_0 constant in the range to 17 MHz. At higher frequencies the field decreased as $1/\omega$ because of the inductivity of the Helmholtz coils.

The plot of the amplitude of the wall velocity $\dot{q}_0 = \omega q_0 = 2\pi\nu q_0$ (q_0 is the wall vibration's amplitude) versus frequency of the field h (Fig. 2) explicitly displays a set of resonant peaks caused by the excitation of the standing flexural waves of the wall.[14] The appropriate dispersion curve of the peak frequency ν_p versus its number n shown in the inset exhibits qualitative agreement with the theory [Eq. (3)]. The experimental value of

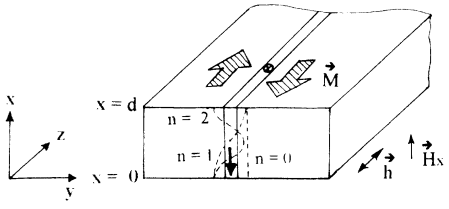

FIG. 1. Geometry of YIG sample containing a single domain wall and schematic view of its flexural modes.

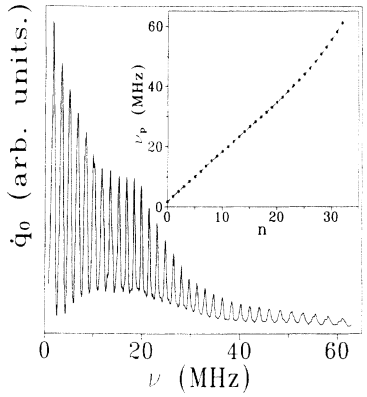

FIG. 2. Amplitude of the wall velocity $\dot{q}_0$ vs frequency ν of ac field h at $H_x = 28$ Oe, $h_0 = 16$ mOe. Inset shows the corresponding plot of the resonant peak frequency ν_p vs its number n.

$c_{\text{expt}} = 2d[\nu_p(n) - \nu_p(n-1)] \approx 100$ m/s obtained at particular conditions is of the same order of magnitude as that calculated from Eq. (3), $c_{\text{cal}} = 120$ m/s (in YIG $Q = 0.05$, $A = 4.2\times10^{-7}$ erg/cm, $\gamma = 17.6$ MHz/Oe). But the exact values of ν_p are strongly dependent on the fields h and H_x.[14,15] In particular, at lower h_0 they increased. Therefore the deviation of the $\nu_p(n)$ plot from a linear one (in the inset of Fig. 2) may be due to the mentioned decrease of drive field at frequencies higher than 17 MHz. Another contribution to the nonlinearity of the dispersion curve may be related to the exchange energy.[5,11]

Note, that we assumed that both even and odd flexural modes $n = 0,1,2,3,\ldots$ were detected by the pickup coil, since the signal from the coil is defined by the integral:

$$I(n,t) \sim \int_0^d \frac{dq_n(x,t)}{dt}dx = \omega\int_0^d q_n(x,t)dx\ ,$$

or, using Eq. (4), we shall obtain at $Q \ll 1$,

$$I(n,t) \sim \frac{2d}{\pi NQ}\sin\left[\frac{\pi nQ}{4}\right]\sin\left[\omega t - \frac{\pi nQ}{4}\right], \qquad I \neq 0 \ \text{ at } 0 \le n < \frac{4}{Q}\ . \tag{6}$$

So, the nonsinusoidal character of the standing waves caused by the spectrum asymmetry at $Q \ll 1$ makes it possible to detect a large number of modes $n \sim 80$ (for YIG). Unfortunately, we could not verify the $I(n)$ dependence experimentally and prove the spectrum asymmetry, because the maximum number of modes observed was about 35. But in the next section we shall present the data on the excitations in the moving wall, which may be another manifestation of the mentioned asymmetry.

III. INTERACTION OF THE TRANSLATION AND FLEXURAL MODES OF THE WALL VIBRATIONS

In order to investigate the elementary excitations spectrum of the moving domain wall, the "interrupted" in-

ductive technique was used [16]. The static equilibrium state of the polarized wall in the sample was defined by the internal gradient field dH/dy of magnetostatic origin, whose value is characterized by the measured restoring force coefficient $\kappa_m = 2MdH/dy \approx 6\times 10^3 \mathrm{g/cm^2\,s^2}$. Therefore, to move the wall at constant velocity V, a sawtooth field $\mathbf{H}\|\mathbf{M}$ was applied. The wall velocity is then $V = 8MH_0/(\kappa_m T)$ (T is the sawtooth field period and H_0 its amplitude). The high-frequency wall vibration amplitude q_0 was selectively measured only during the short pulses triggered by the field H signal (see Fig. 3) using an apparatus with a specially designed electronic interrupter.

The plots $\dot{q}_0(v)$, measured at different wall velocities and analogous to that in Fig. 2 showed a clear asymmetry with respect to V. The corresponding dispersion curves ν_p vs n display the same property of the resonant frequencies $\nu_p(V) \neq \nu_p(-V)$ [Fig. 4(a)]. The dispersion remains linear and the slope of the $\nu_p(n)$ curve monotonously decreases when the velocity changes from $-V$ to $+V$. These points are also illustrated by $\nu_p(V)$ plots of different peaks [Fig. 4(b)]. The transition from the monotonous decreasing to increasing curve occurred when the wall polarity was reversed by the dc field H_x (the magnetization in domains was ascertained to be unchanged). Another important observed point is that more high-frequency peaks were successively suppressed at higher $|V|$. This point is seen in the plots of the peak width $\Delta\nu$ at the 0.7 level versus its number n and $\Delta\nu$ vs V at different n (Fig. 5). These data also display the asymmetric dependence on V.

The data on the wall resonance linewidth yield information on the magnon damping parameter in the moving wall. At low velocities the damping was found to be approximately equal to that found from FMR, as in Refs. 13 and 14. But at higher $|V|$, the dispersive dependence of damping on the wave vector arises [$\sim n^2$, see Fig. 5(a)]. The dispersion of damping, first of all, may be due to the multimagnon scattering processes.[1,20] The second reason is related to the interaction of the wall magnons and different types of nonlinear excitations of the wall structure, their number being larger at higher $|V|$. They

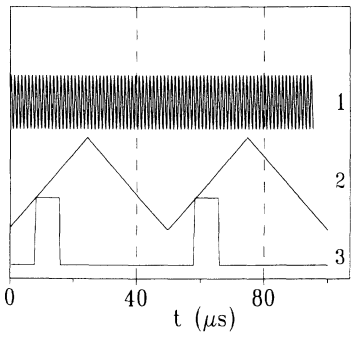

FIG. 3. Illustration of "interrupted" technique. Real-time signals of the high-frequency field h (1) and low-frequency field H (2). The wall motion was recorded during short pulses (3).

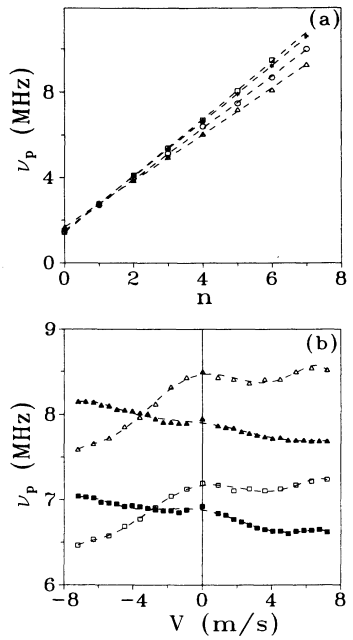

FIG. 4. Plots of the peak frequency ν_p vs (a) its number n, obtained by "interrupted" technique at different $V = -7.2$ m/s (□), $V = 0$ m/s (*), $V = 2.7$ m/s (○) and $V = 7.2$ m/s (△), and (b) the wall velocity V of different peaks $n = 4$ (□■), $n = 5$ (△▲) at $H_x = 28$ Oe (■▲), and $H_x = -28$ Oe (□△), $h_0 = 19$ mOe.

were revealed in these conditions magneto-optically, using single-sweep traces on the storage oscilloscope as in Refs. 17 and 18.

The observed asymmetric dependences of the flexural

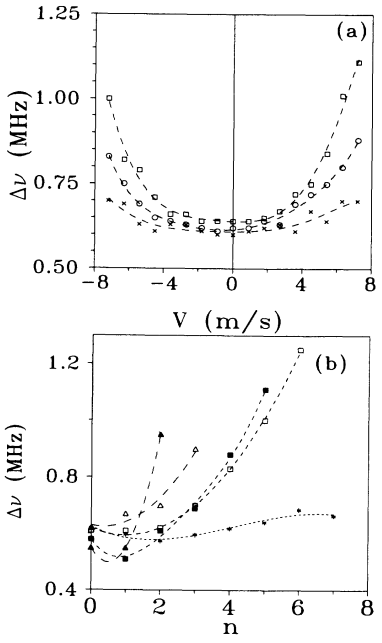

FIG. 5. Curves of the peak width $\Delta\nu$ at the 0.7 level vs (a) n at different wall velocities $V = 6.3$ m/s (▲), $V = -6.3$ m/s (△), $V = 5$ m/s (■), $V = -5$ m/s (□), $V = 0$ m/s (*), $H_x = 28$ Oe; and (b) V at $n = 2$ (*), $n = 3$ (○), $n = 4$ (□). $h_0 = 19$ mOe, $H_x = 28$ Oe.

mode eigenfrequencies and resonance linewidths (hence the phase velocity and damping) on the wall velocity contradicts the theories[7,12] that were developed for the high-anisotropy ferromagnets $Q \gg 1$, when $c_+ = c_- = c_0$. Therefore, we believe that these effects are definitively related to the asymmetry of the spectrum itself, $c_+ \neq c_-$, which was predicted for the stationary wall in the low-anisotropy ferromagnets. Unfortunately, no such theory exists for the moving wall now.

In addition to the wall motion influence on the excitation spectrum, the opposite effect, of the wall excitation influence on the translation motion, was also observed. Using a spectrum analyzer and a lock-in amplifier, we simultaneously measured the amplitude of the forced low- and high-frequency wall vibrations (q_l and q_h) caused by the fields H and h, respectively. The plots $\dot{q}_l(\nu)$ and $\dot{q}_h(\nu)$ exhibit the peaks at the same resonant frequencies (Fig. 6). The magnitude of $\dot{q}_l$ was nearly proportional to H. The phase of the low-frequency signal was found to be nearly constant at any ν values. Therefore, the field h did not affect markedly the low-frequency wall mobility. So, we conclude that the peaks observed in the $\dot{q}_l(\nu)$ curves are essentially due to the change of the local restoring force coefficient κ_{loc} (thus the total value $\kappa = \kappa_m + \kappa_{\text{loc}}$) of the wall. This change may be described by allowing for the magnetic after-effect caused by the interaction of the moving wall with dynamic defects, whose energy depends on the local magnetization (e.g., the electron jumps $Fe^{2+} \leftrightarrow Fe^{3+}$).[21] The low-amplitude wall vibrations, due to the influence of such a local induced anisotropy near the wall, will occur in a deeper potential well than high-amplitude ones at resonant frequencies of the field h. Note, that, in case the inverse relaxation time τ^{-1} of the defects is of the same order as the frequency ν of the field h, only this field changes the magnitude of κ. Therefore, the value of $q_l \sim H/\kappa$ will also be larger at resonant frequencies ν_p.

Another possible reason lies in the interaction of the wall with static defects, distributed over the sample (not locally near the wall as in the previous case). Then the κ value will be determined by the ratio of h and mean coercive field of a defect.

This two-frequency technique can be a useful tool for the investigation of the other types of the wall excitations as well. In particular, we observed a similar phenomenon in two-frequency oscillations of a single Bloch line in a "demagnetized" wall ($H_x = 0$).[22]

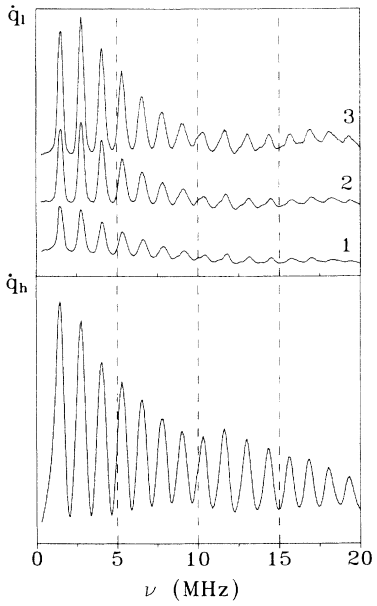

FIG. 6. Plots of the velocity amplitude of forced low- and high-frequency wall vibrations ($\dot{q}_l$ and $\dot{q}_h$) vs frequency ν at $h_0 = 15$ mOe, $H_x = 28$ Oe, low-frequency field $H_0 = 14$ mOe (1), 22 mOe (2), 29 mOe (3), $\Omega = 20$ kHz.

IV. INSTABILITIES OF DOMAIN-WALL EXCITATIONS

The spin-wave instabilities and chaotic behavior of parametrically excited magnons in magnets without domain walls have been intensively studied in recent years.[3] In this section we shall describe a number of nonlinear effects in the wall excitation experiments.

Figure 7 shows the graph of the amplitude of the wall velocity $\dot{q}_0$ versus drive field amplitude h_0 at the given frequency $\nu = 0.94$ MHz. Three regions corresponding to different regimes of the wall motion and separated by two points of instability are clearly seen. In region 1 the linear wall vibrations take place and their Fourier-transform spectrum contains only the first harmonic at the field h frequency. But at some threshold value $h_{t1} \approx 10$ mOe a drastic rise of $\dot{q}_0$ occurs, accompanied by the appearance of the upper harmonics and of the narrow bands of the continuous spectrum. These bands correspond to the excitation of the flexural modes, as can be seem from a comparison of the Fourier spectrum $F_{\dot{q}}(f)$ and the $\dot{q}_0(\nu)$ curve (Fig. 8). Another demonstration is that a dc field H_x change, which caused the displacement of the peaks in the $\dot{q}_0(\nu)$ curves, resulted in the corre-

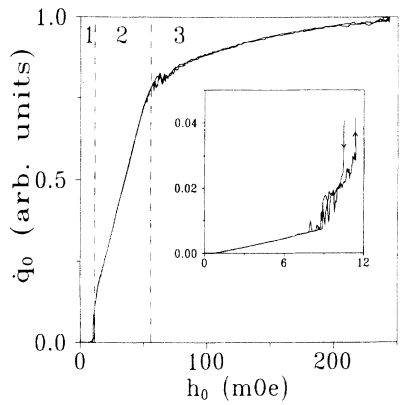

FIG. 7. Dependence of the wall velocity amplitude $\dot{q}_0$ on the field amplitude h_0 at $H_x = 28$ Oe and $\nu = 0.94$ MHz. Inset shows the initial region of the curve.

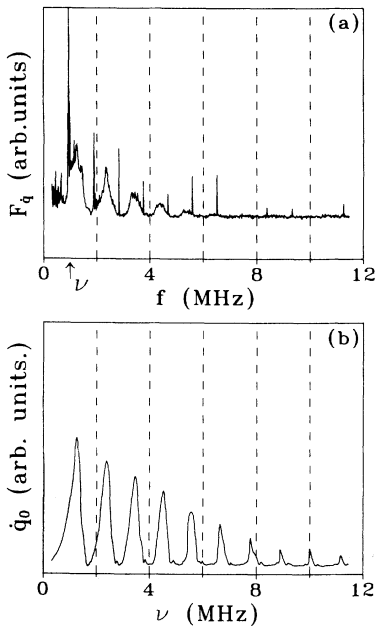

FIG. 8. (a) Fourier-transform spectrum $F_{\dot{q}}(f)$ of the wall vibrations signal at $\nu=0.94$ MHz, $h_0=34$ mOe; and (b) frequency dependence of the wall velocity amplitude $\dot{q}_0(\nu)$ at $h_0=23$ mOe; $H_x=28$ Oe.

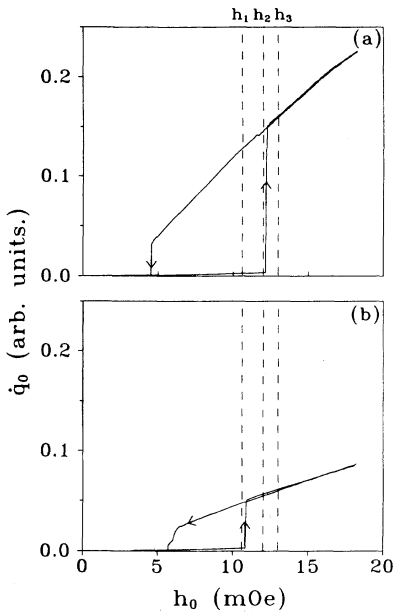

FIG. 10. Graphs of $\dot{q}_0(h_0)$ like those in Fig. 7, recorded at (a) $\nu=\nu_1=1.2$ MHz and (b) $\nu=\nu_2=2.3$ MHz. The fields h_1, h_2, h_3 marked by vertical dashed lines, correspond to the plots (a)–(c) in Fig. 9. The frequencies ν_1 and ν_2 are marked the same as in Fig. 9.

sponding change of the Fourier spectrum.

The unstable growth of the wall vibration amplitude q_0 at the first instability point has an effect on the $\dot{q}_0(\nu)$ curves (see Fig. 9), resulting in the disappearance of the lower resonances. The curves recorded at increasing (solid line) or decreasing (dashed line) frequency exhibit hysteresis behavior. Figure 10 shows hysteresis plots $\dot{q}_0(h_0)$ like those in Fig. 7, measured at different frequencies ($\nu=\nu_1=1.2$ MHz and $\nu=\nu_2=2.3$ MHz), being in a good agreement with $\dot{q}_0(\nu)$ graphs [vertical dashed lines in Fig. 9 correspond to $\dot{q}_0(h_0)$ curves *a* and *b* in Fig. 10, and *vice versa;* the similar lines in Fig. 10 correspond to plots *a*, *b*, and *c* in Fig. 9). Thus the failure of the lower modes in $\dot{q}_0(\nu)$ curves at decreasing field is definitively related to the transition from the high- to low-mobility region through the hysteresis area in the $\dot{q}_0(h_0)$ plot.

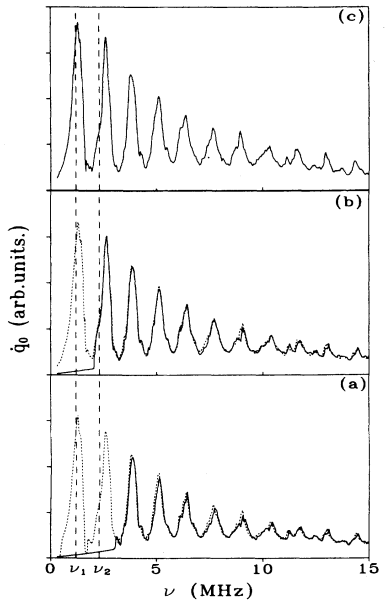

FIG. 9. Plots $\dot{q}_0(\nu)$ at (a) $h_0=10.6$ mOe, (b) 12 mOe, and (c) 13 mOe. Solid curves were recorded at increasing ν and dashed curves, at decreasing ν.

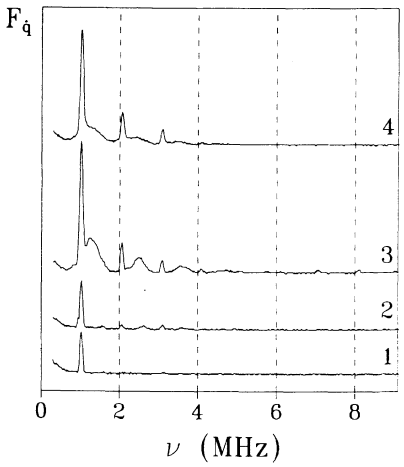

FIG. 11. Fourier-spectra of the wall oscillations caused by the simultaneous action of the high-frequency field $h_0=7$ mOe, $\nu=1.02$ MHz and low-frequency field H (at $\Omega=5$ kHz) at different wall velocities V ($V=8M\Omega H_0/\kappa_m$): 0 m/s (1), 0.16 m/s (2), 0.5 m/s (3), 1.44 m/s (4). $H_x=28$ Oe.

The phenomenon of the threshold excitation of flexural modes was also observed in experiments with a translationally moving wall. The small high-frequency ($\nu=1.02$ MHz) field $h_0<h_{t1}$ and the low-frequency ($\Omega=5$ kHz) sawtooth field $\mathbf{H}\|\mathbf{M}$, which caused the wall to move at constant velocity V, were applied simultaneously. Fourier spectra corresponding to different V (Fig. 11) show the appearance of the same flexural modes at some threshold velocity value $V_t=0.5$ m/s (it was determined by the magnitude of h_0). In this case the phenomenon was less developed. In order to enhance the signal-to-noise ratio, we used the larger resolution bandwidth ($W=10$ kHz) of the spectrum analyzer than earlier (in Fig. 8 $W=100$ Hz). Therefore the discrete harmonics in Fig. 11 have a larger visible linewidth than those in Fig. 8. One other distinction is that the fine structure of the multiple harmonics exists in the present case. A number of peaks at combined frequencies $\nu_c=n\nu\pm m\Omega$ ($n,m=1,2,3,\ldots$) are clearly seen (Fig. 12).

In these experiments the wall was displaced by the low-frequency field at a large distance. Therefore we conclude that the threshold excitation of flexural modes cannot be attributed to the interaction with static defects. A more probable reason may be the after-effect phenomenon, discussed in the previous section. The parametric excitation of the wall magnons, like that in the bulk spin-wave experiments is also a possible explanation [3]. So, the nonlinear theory of the spin-wave instabilities and chaos in a domain wall is required.

Now, we shall discuss the experimental manifestation of the chaotic behavior of the wall at the second instability. It occurs at higher h_0 when the wall mobility drastically decreases. It is a transition from region 2 to region 3 in Fig. 7. This instability is characterized by changes in the real-time signals of the wall vibrations from periodic to chaotic [see Fig. 13(a)]. In the Fourier-spectrum a large continuous component appears with a noisy discrete harmonics at the frequencies $\nu_n=(n+\frac{1}{2})\nu$ [Fig. 13(b)]. Using the signal from the pickup coil $\sim\dot{q}$ and the numerically integrated one, we obtained the phase-space trajectories $\dot{q}$ vs q. Figure 13(c) displays the explicit bifurcation from the periodic pattern to the chaotic pattern, like a chaotic strange attractor. A more detailed experimental study of the chaotic dynamics of a domain wall will be published elsewhere.

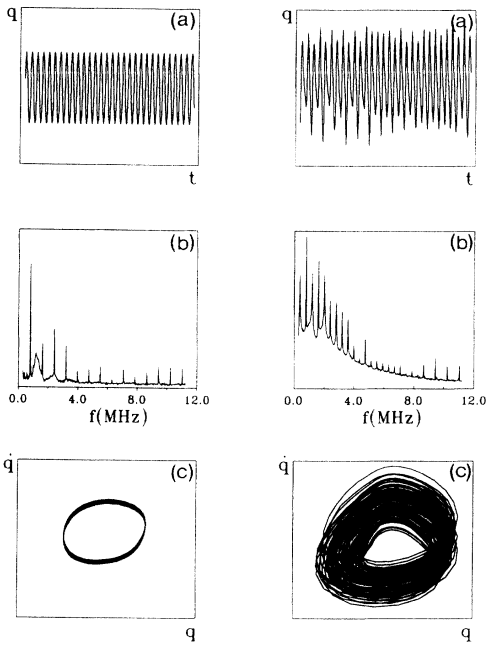

FIG. 13. (a) Real-time signals, (b) Fourier-spectra, and (c) phase portraits of the wall vibrations caused by the field $h_0=45$ mOe (left plots) and $h_0=0.3$ Oe (right plots). $\nu=0.79$ MHz, $H_x=28$ Oe.

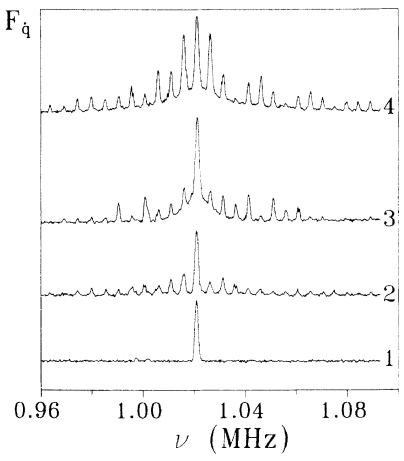

FIG. 12. Fine structure of the first harmonic in Fig. 11.

It should be noted that the transition to the chaotic regime of the wall motion was accompanied by a dynamic structure conversion. It consisted of chaotic nucleation, motion, and annihilation of the nonlinear excitations of the wall structure: "dynamic" subdomains—Bloch lines pairs (like breathers), and small subdomain nuclei localized near the sample surfaces (like low-amplitude solitons). These excitations were often transformed to a static surface subdomain nucleus, or even pairs of Bloch lines after switching off the field. But the repeat switch-on of the smaller ac field moved them out of the sample and the wall became polarized. A detailed magneto-optic study of such excitations in YIG was carried out in the previous works.[14,15,17,18] Thus the process of interaction of elementary and nonlinear excitations, in fact, defines both the quantitative parameters of the wall motion—velocity or mobility, and qualitative features—the periodic or chaotic character of the motion.

V. CONCLUSIONS

The present experiments show that a domain wall in YIG is a suitable system for the investigation of various branches of spectrum of magnetic excitations. The magnons in a moving domain wall are found to possess unexpected asymmetric properties with respect to the wall velocity, which have no analogs in other types of excitations in solids. Nonlinear phenomena of threshold exci-

tation of flexural waves are found to take place both in the moving wall and in the wall at rest. Finally, the experimental techniques that have been described enable the determination of detailed information on a variety of elementary and nonlinear excitations of different dimensions and on the complex chaotic dynamics of a two-dimensional spin system. Unfortunately, an appropriate nonlinear theory is still lacking.

[1]M. Sparks, *Ferromagnetic Relaxation Theory* (McGraw-Hill, New York, 1964).

[2]A. I. Akhiezer, V. G. Baryakhtar, and V. S. Peletminskii, *Spin Waves* (North-Holland, Amsterdam, 1968).

[3]S. M. Rezende and F. M. De Aguiar, Proc. IEEE **78**, 893 (1990), and references therein.

[4]A. P. Malozemoff and J. C. Slonczewski, *Magnetic Domain Walls in Bubble Materials* (Academic, New York, 1979).

[5]J. M. Winter, Phys. Rev. **124**, 452 (1961).

[6]J. F. Janak, Phys. Rev. **134**, A411 (1964).

[7]A. A. Thiele, Phys. Rev. B **7**, 391 (1973).

[8]I. A. Gilinskii, Zh. Eksp. Teor. Fiz. **68**, 1032 (1975) [Sov. Phys. JETP **41**, 511 (1975)].

[9]A. E. Borovik, V. S. Kuleshov, and M. A. Strzemechnyi, Zh. Eksp. Teor. Fiz. **68**, 2236 (1975) [Sov. Phys. JETP **41**, 1118 (1985)].

[10]Yu. A. Dimashko, P. P. Shatskii, and D. A. Yiablonskii, Fiz. Tverd. Tela (Leningrad) **30**, 3084 (1988) [Sov. Phys. Solid State **30**, 1774 (1988)].

[11]A. V. Mikhailov and V. S. Shimokhin, Zh. Eksp. Teor. Fiz. **97**, 1966 (1990) [Sov. Phys. JETP **70**, 1109 (1990)].

[12]Yu. I. Gorobetc, V. I. Finokhin, and Yu. I. Jejerya, Ukr. Fiz. Zhur. (Sov. Ukr. Phys. Journ.) **36**, 1215 (1991).

[13]J. C. Slonczewski, B. E. Argyle, and J. H. Spreen, IEEE Trans. Magn. **MAG-17**, 2760 (1981).

[14]L. M. Dedukh, V. I. Nikitenko, and V. T. Synogach, Zh. Eksp. Teor. Fiz. **94**, 312 (1988) [Sov. Phys. JETP **67**, 1912 (1988)].

[15]L. M. Dedukh, V. I. Nikitendo, and V. T. Synogach, Acta Phys. Pol. A **76**, 295 (1989).

[16]V. T. Synogach, Pis'ma Zh. Eksp. Teor. Fiz. **53**, 369 (1991) [JETP Lett. **53**, 387 (1991)].

[17]V. S. Gornakov, L. M. Dedukh, and V. I. Nikitenko, Pis'ma Zh. Eksp. Teor. Fiz. **39**, 199 (1984) [JETP Lett. **39**, 236 (1984)].

[18]V. I. Nikitenko, L. M. Dedukh, V. S. Gornakov, and V. T. Synogach, in *Proceedings of the Third International Conference on the Physics of Magnetic Materials* (Poland, 1986), edited by W. Gorzkowski, H. K. Lachowicz, and H. Szymczak (World Scientific, Singapore, 1986).

[19]A. V. Mihkahilov and V. S. Shimokhin (unpublished).

[20]V. I. Butrim, B. A. Ivanov, and Yu. N. Mitcai, Fiz. Tverd. Tela (Leningrad) **29**, 268 (1987) [Sov. Phys. Solid State **29**, 154 (1987)].

[21]A. Hubert, *Theorie der Domanewande in geordneten Medien* (Springer-Verlag, Berlin, 1974).

[22]V. S. Gornakov, V. I. Nikitenko, and V. T. Synogach, in Proceedings of the International Symposium on Magneto-Optics (Kharkov, 1991) [Fiv. Nizk. Temp. (Sov. Low-Temp. Phys.) (to be published)].